Supplementary Information (SI) for EES Batteries.

Electrode surface engineering with electrolyte additives, improving reversibility of magnesium metal anode batteries

Muath Radi[1]*, Deyana S. Tchitchekova[2], Alexandre Ponrouch[2]* and Rémi Dedryvère[1,3]*

[1] IPREM, Université de Pau & Pays Adour, CNRS UMR 5254, E2S-UPPA, 64000, Pau, France

[2] Institut de Ciencia de Materials de Barcelona, ICMAB-CSIC, Campus UAB, 08193, Bellaterra, Spain

[3] RS2E, Réseau sur le Stockage Electrochimique de l'Energie, FR CNRS 3459, France

* E-mail: muath-m-m.radi@univ-pau.fr, remi.dedryvere@univ-pau.fr, aponrouch@icmab.es.

Table S1: Summary of the additives used with $Mg(TFSI)_2$ electrolyte.

Electrolyte	Cycling Conditions	Voltage Hysteresis	Coulombic Efficiency
0.5 M $MgTFSI_2$ + 2 wt. %HpMS in TG [7]	CV, WE: Pt, scan rate: 20 mV s^{-1}	2 V (without HpMS) 0.4 V (with HpMS)	First cycle: 18.4%, improving over cycling (without HpMS). First cycle: 66.2%, retained over cycling (with HpMS)
0.1 M $Mg(TFSI)_2$ + 130 mM of $Mg(butyl)_2$ in DME:DG [5]	CV (cycles 1 to 100) WE: Ti, scan rate: 25 mV s^{-1}.	87% after 20 cycles	< 50 mV at the first cycle, ~180 mV after the 20th cycle
0.5 M $Mg(TFSI)_2$ + 0.5 M 18C6 in THF [8]	CV, WE: Pt, scan rate: 1 mV s^{-1}.	No redox current was observed (without 18C6) ~ 2 V (with 18C6)	27% (with 18C6)
0.5 M $Mg(TFSI)_2$ + 0.5 M NCCN·2HCl in DME [10]	CV, WE: SS, Galvanostatic charge/discharge of Mg||Mg symmetry	~ 95 % in Mg||SS half cells	(< 0.2 V) in Mg||Mg symmetry cells

	cells.		
0.4 M $Mg(TFSI)_2$ + 0.1 M $Mg(BH_4)_2$ in diglyme [11]	CV, WE: Pt, scan rate: 20 mV s^{-1}	98.8%	0.25 V
0.5 m $Mg(TFSI)_2$ + 50 mM I_2 in DME [13]	Galvanostatic charge/discharge tests; Mg/Mg/Mg (T) Swagelok-cell	Not reported	2.67 V (without Iodine) 0.22 V (with Iodine)

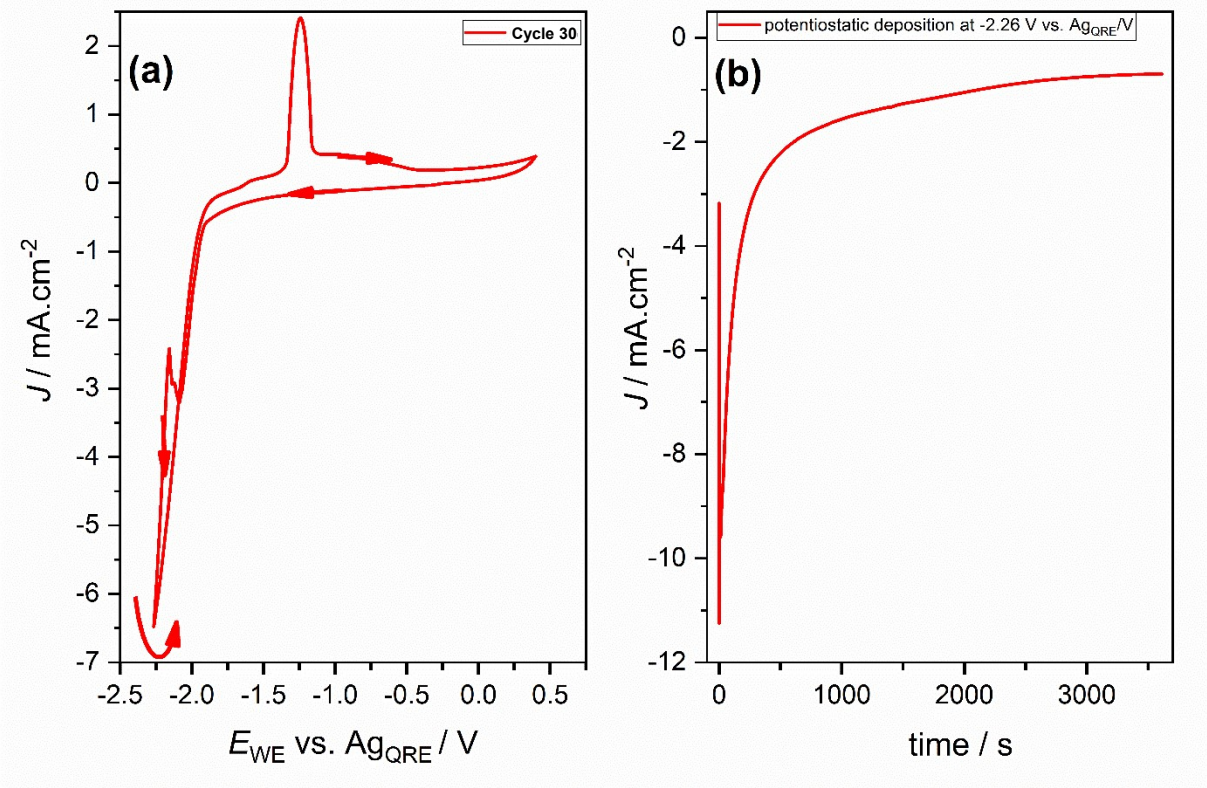

Figure S1: (a) Cyclic voltammograms (30th cycle) of a Ti electrode with a scan rate of 25 mV/s using 0.4 M $Mg(TFSI)_2$ in DME:DG electrolyte with 8 wt.% of BF_3·DE. The CV was stopped after a stripping scan, then (b) 1 hour of Mg potentiostatic deposition at -2.26 V *vs.* Ag_{QRE} was applied.

Table S2: Binding energy (E_B) and atomic percentage (at.%) of the components observed in XPS spectra reported in Figures 2 and S2 of the Mg deposits formed on a Ti substrate.

	0.4 M Mg(TFSI)2 after 50th plating scan (Fig. 2 e) [5]		0.4 M $Mg(TFSI)_2$ + 1.5 wt.% BF_3·DE after 50th plating scan (Fig. 2 a)		4 M $Mg(TFSI)_2$ + 4 wt.% BF_3·DE after 50th plating scan (Fig. 2 b)		0.4 M $Mg(TFSI)_2$ + 8 wt.% BF_3·DE after 50th plating scan (Fig. 2 c)		0.4 M $Mg(TFSI)_2$ + 8 wt.% BF_3·DE after 33rd stripping scan + 1-hour PSD (Fig. 2 d)		
Core peak	**E_B (eV)**	**at.%**	**E_B (eV)**	**at.%**	**E_B (eV)**	**at.%**	**E_B (eV)**	**at.%**	**E_B (eV)**	**at.%**	**Chemical attribution**
Mg 2p	48.4	0.2							48.5	2.0	Mg^0
	50.7	20	51.7	22	51.7	22	51.8	19	51.2	20	Mg^{2+}
S $2p_{3/2}$	161.1	1.3							161.5	0.3	Mg**S**
	162.5	0.8	161.9	0.5	162.1	0.1	162.5				Mg$\mathbf{S}_n$ (terminal S)
	167.5	0.6	166.8	0.1	167.7	0.1	167.9	0.3	167.4	0.1	sulfite
	169.2	2.7	169.5	2.1	169.7	2.1	169.8	3.4	169.5	2.5	TFSI
B 1s			188.3	0.3	188.5	0.3	189.1	0.8	188.3	1.0	MgB_2
									192.0	2.1	B in oxygen environment
			192.8	2.4	193.2	1.7	192.9	1.4	192.9	1.5	
					195.5	0.2	195.7	0.2			BF_xO_y
C 1s	285.0	9.9	285	3.9	285.0	2.7	285.0	3.2	285.0	3.3	CH_x
	286.6	5.4	287.1	6.4	187.1	6.0	287.2	6.0	287.1	7.9	CO
	288.6	1.2	288.7	1.1	288.6	0.9	289.0	0.8	289.1	0.6	O–C=O
	290.3	2.5							290.5	0.3	$MgCO_3$
	292.9	1.9	293.3	1.7	293.3	2	293.5	3.3	293.4	2.1	TFSI
O 1s	530.0	1.8							529.8	2.5	MgO
	531.5	11							531.5	7.0	MgO
	532.4	16	532.5	8.0	532.6	6.2	533.0	6.2	532.6	11	CO_x
	533.5	6.4	533.8	4.7	533.8	4.5	533.7	5.9	533.8	6.8	TFSI
F 1s	685.6	6.2	685.9	38	685.9	42	686.1	36	686.0	18	MgF_2
	688.9	9.5	689.0	7.3	689.0	7.4	689.2	12	689.1	9.9	TFSI

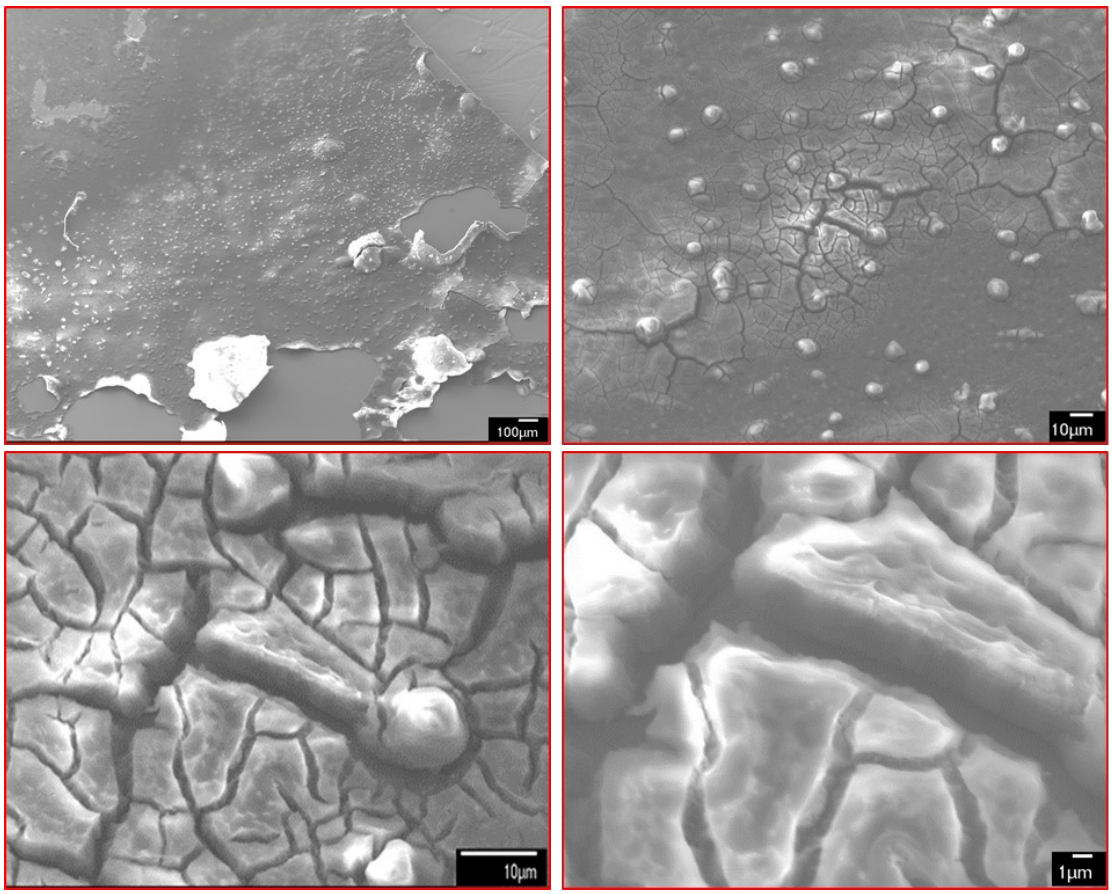

Figure S2: Scanning electron microscopy images of Mg deposits formed on Ti electrodes cycled in 0.4 M $Mg(TFSI)_2$ in DME:DG electrolyte with 8 wt.% of BF_3·DE after 30th stripping scan followed by 1 hour of Mg potentiostatic deposition at – 2.26 V *vs.* Ag_{QRE} (from Figure S1).

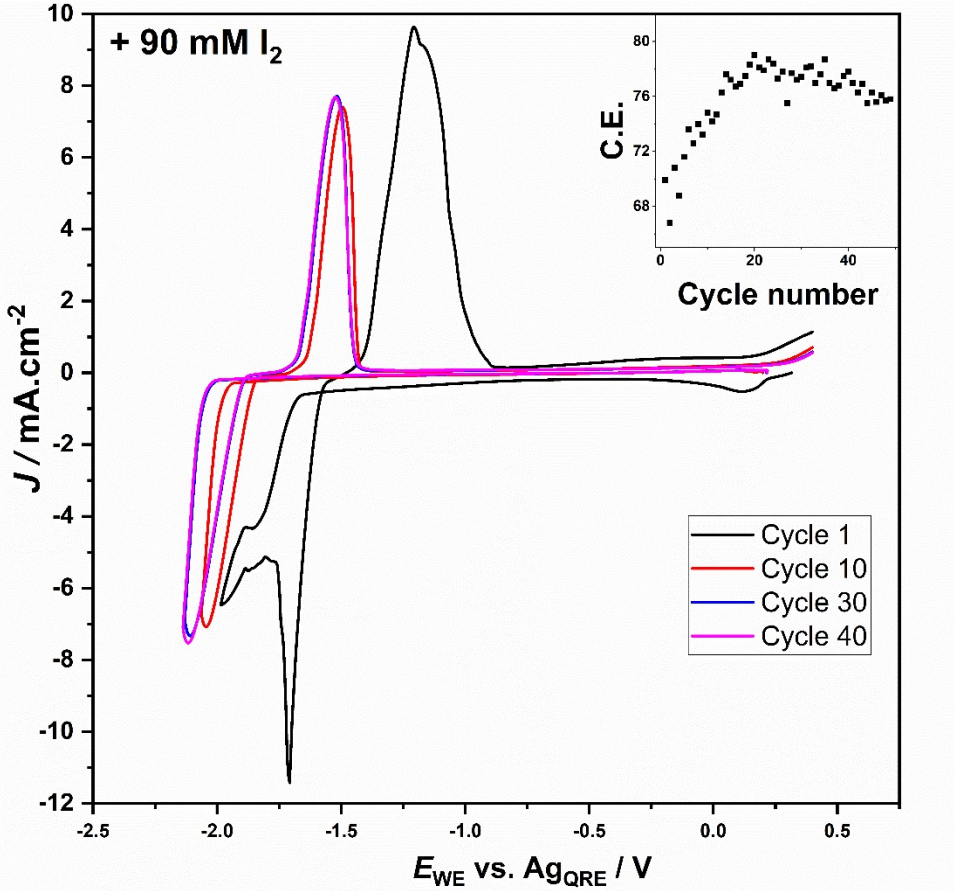

Figure S3: Cyclic voltammograms of a Ti electrode with a scan rate of 25 mV/s at several cycle numbers using 0.4 M $Mg(TFSI)_2$ in DME:DG electrolyte, with adding 90 mM of I_2.

Table S3: Binding energy (E_B) and atomic percentage (at.%) of the components observed in XPS spectra reported in Figure 4 of the Mg deposits formed on a Ti substrate.

	0.4 M $Mg(TFSI)_2$ + 10 mM I_2 after 50th plating scan (Fig. 4 a)		0.4 M $Mg(TFSI)_2$ + 20 mM I_2 after 50th plating scan (Fig. 4 b)		0.4 M $Mg(TFSI)_2$ + 40 mM I_2 after 50th plating scan (Fig. 4 c)		
Core peak	**E_B (eV)**	**at.%**	**E_B (eV)**	**at.%**	**E_B (eV)**	**at.%**	**Chemical attribution**
Mg 2p	51.2	11	50.7	20	50.7	13	Mg^{2+}
S 2p$_{3/2}$	161.9	0.5	161.3	0.9	161.0	0.6	MgS
	164.3	0.2	162.9	0.4	162.4	0.6	
	167.9	0.4	167.0	0.3	168.3	0.5	decomposition of the salt
	169.8	6.8	169.1	3.3	169.5	2.1	TFSI
C 1s	285	8.4	285.0	9.3	285.0	4.3	CH_x
	287.3	8.8	286.7	11	286.8	13	CO
			288.3	0.8	289.1	0.8	O–C=O
	290.4	0.5	290.3	1.3	290.2	1.3	$MgCO_3$
	293.5	5.7	293.0	2.6	293.1	1.5	TFSI
N 1s					397.5	0.2	TiN
	400.0	3.4	399.3	2.6	399.4	2.3	TFSI, organic N
Ti 2p$_{3/2}$					454.6	0.04	TiN
					457.1	0.1	Ti_2O_3
					459.1	0.6	TiO_2
O 1s					530.0	1.8	TiO_2
	531.8	4.9	531.4	9.3	531.6	12	MgO
	532.6	11	532.3	16	532.4	19	CO_x
	533.7	13	533.6	6.3	533.9	4.9	TFSI
I 3d$_{5/2}$	619.5	0.2	619.0	0.6	619.1	1.3	MgI_2
F 1s	685.9	4.1	685.4	8.1	685.6	5.8	MgF_2
	689.2	21	688.7	11	689.1	7.8	TFSI

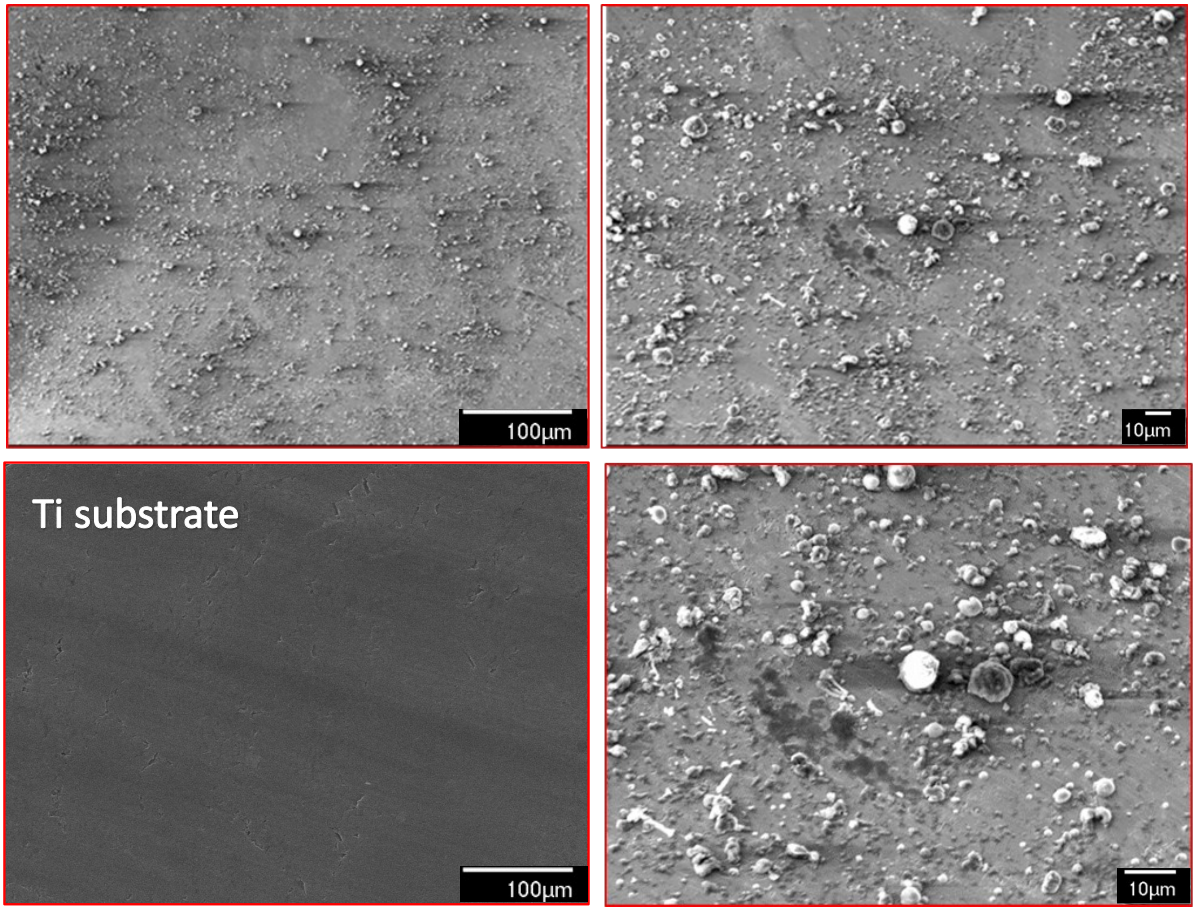

Figure S4: Scanning electron microscopy images of Mg deposits formed on Ti electrodes cycled in 0.4 M $Mg(TFSI)_2$ electrolyte with adding 40 mM I_2 at the end of the 50^{th} plating scan (Figure 4c) and the pristine Ti substrate.

Table S4: Binding energy (E_B) and atomic percentage (at.%) of the components observed in XPS spectra reported in Figure 6 of the Mg deposits formed on a Ti substrate.

	0.4 M $Mg(TFSI)_2$ + 10 mM BI3 after 50th plating scan (Fig. 6 a)		0.4 M $Mg(TFSI)_2$ + 20 mM BI_3 after 50th plating scan (Fig. 6 b)		0.4 M $Mg(TFSI)_2$ + 40 mM BI_3 after 50th plating scan (Fig. 6 c)		
Core peak	**E_B (eV)**	**at.%**	**E_B (eV)**	**at.%**	**E_B (eV)**	**at.%**	**Chemical attribution**
Mg 2p	50.6	16	50.5	18	50.7	13	Mg^{2+}
S $2p_{3/2}$	161.6	1.1	161.5	0.6	161.7	0.5	MgS
	168.2	0.6	167.8	0.4	167.5	0.3	decomposition of the salt
	169.4	3.9	169.4	3.5	169.5	3.6	TFSI
B 1s	192.3	0.7	192.1	1.1	192.5	3.2	B in oxygen environment
C 1s	285.0	5.2	285.0	6.0	285.0	8.7	CH_x
	287.0	10	287.0	7.1	287.0	12	CO
	289.3	0.6	289.3	0.9	289.5	1.1	O–C=O
	290.3	1.5	290.4	0.6			$MgCO_3$
	293.2	3.5	293.2	2.9	293.3	3.0	TFSI
N 1s	399.2	2.8	399.1	2.3	400.0	2.2	TFSI, organic N
Ti $2p_{3/2}$			453.9	0.1	454.3	0.1	Ti^0
			455.2	0.1	455.4	0.1	TiN
	457.5	0.2	457.3	0.8	457.5	0.5	Ti_2O_3
	459.2	0.4	459.1	1.4	459.3	1.1	TiO_2
O 1s	530.2	2.1	530.2	4.7	530.4	2.2	TiO_2
	531.6	9.9	531.6	15	531.6	11	MgO
	532.5	16	532.5	12	532.6	14	CO_x
	533.7	7.7	533.6	7.2	533.8	7.7	TFSI
I $3d_{5/2}$	619.2	0.8	619.2	1.1	619.3	2	MgI_2
F 1s	685.6	4.4	685.7	2.7	685.7	2.9	MgF_2
	689.1	13	689.1	12	689.2	12	TFSI

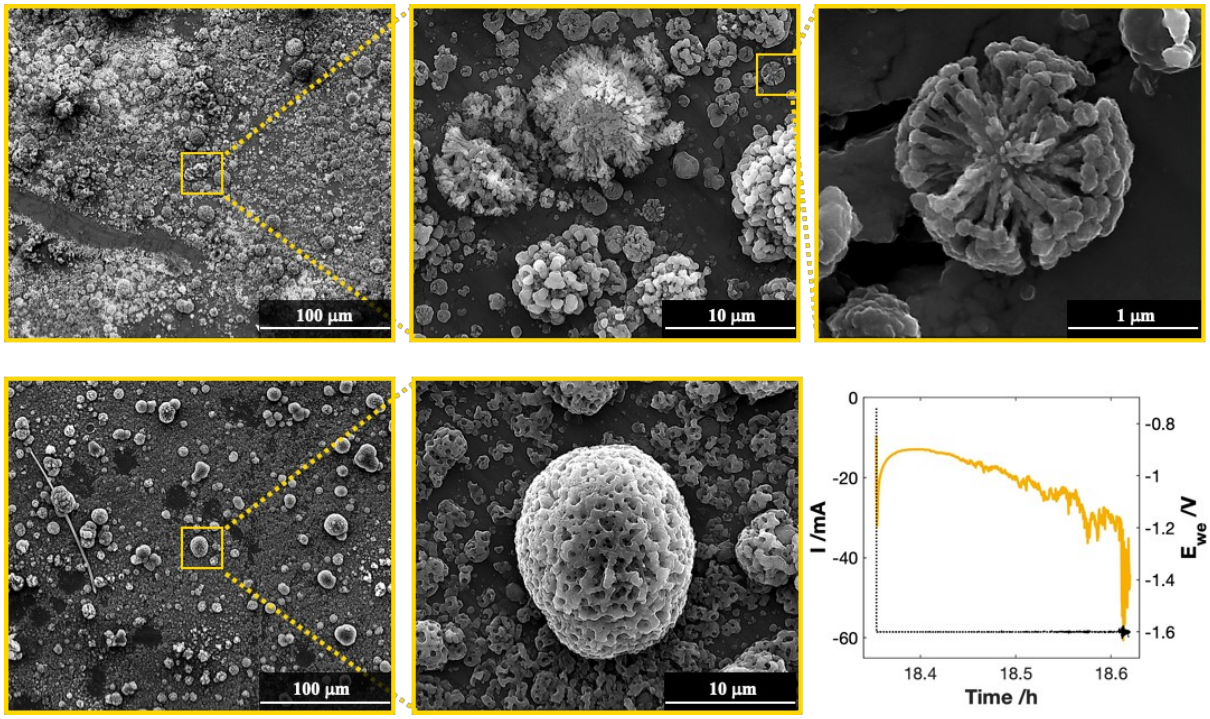

Figure S5: Scanning electron microscopy (SEM) images of Mg deposits formed on Ti electrodes cycled in 0.4 M $Mg(TFSI)_2$ electrolyte containing 40 mM BI_3. Mg electrodeposition was performed potentiostatically at -1.6 V *vs.* Mg^{2+}/Mg after the full cycling protocol described in the Experimental Section. The top row presents micrographs acquired at increasing magnification near the edge of the Ti electrode. At low magnification, the surface is covered by heterogeneous deposits, including large spherical agglomerates (≥10 µm) and smaller dispersed particles. Higher magnification reveals that these agglomerates consist of clusters of smaller spherical subparticles with a cauliflower-like morphology, while flower-like radially arranged crystallites (~1–2 µm) are also locally observed. The bottom row shows images from the central region of the same electrode, where deposits appear predominantly as isolated spherical particles (≥10 µm) with a highly porous and interconnected, sponge-like texture (middle image). The final panel displays the current–time response recorded during the potentiostatic deposition step (~16 min). Notably, despite the relatively high current reached during deposition (>60 mA), no dendritic structures were observed in the SEM analysis.

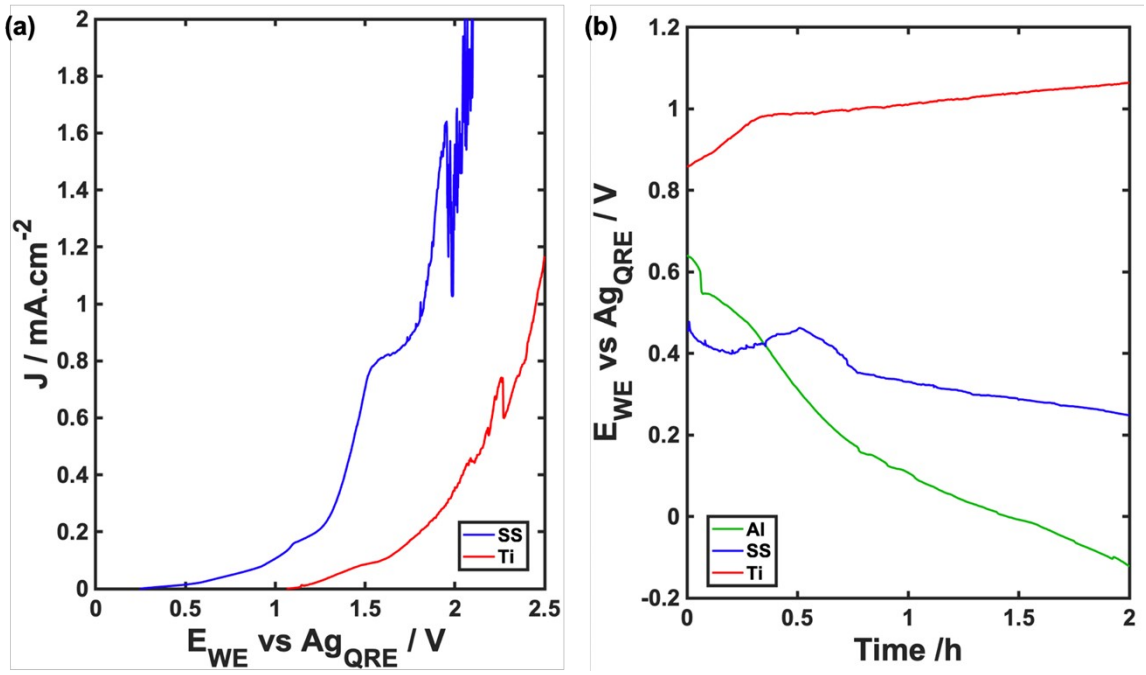

Figure S6: (a) LSV of SS and Ti electrodes with a scan rate of 0.1 mV/s using 0.4 M $Mg(TFSI)_2$ in DME:DG electrolyte with 40 mM of BI_3 *vs.* Ag_{QRE}. Oxidative onsets are at ~1.5 V *vs.* Ag^+/Ag for Ti and ~1.0 V *vs.* Ag^+/Ag for SS, confirming Ti is a more electrochemically inert substrate under anodic polarization in this electrolyte formulation. (b) Open circuit potential equilibration on Al, SS, and Ti electrodes for 2 hours before the LSV experiments in (a).

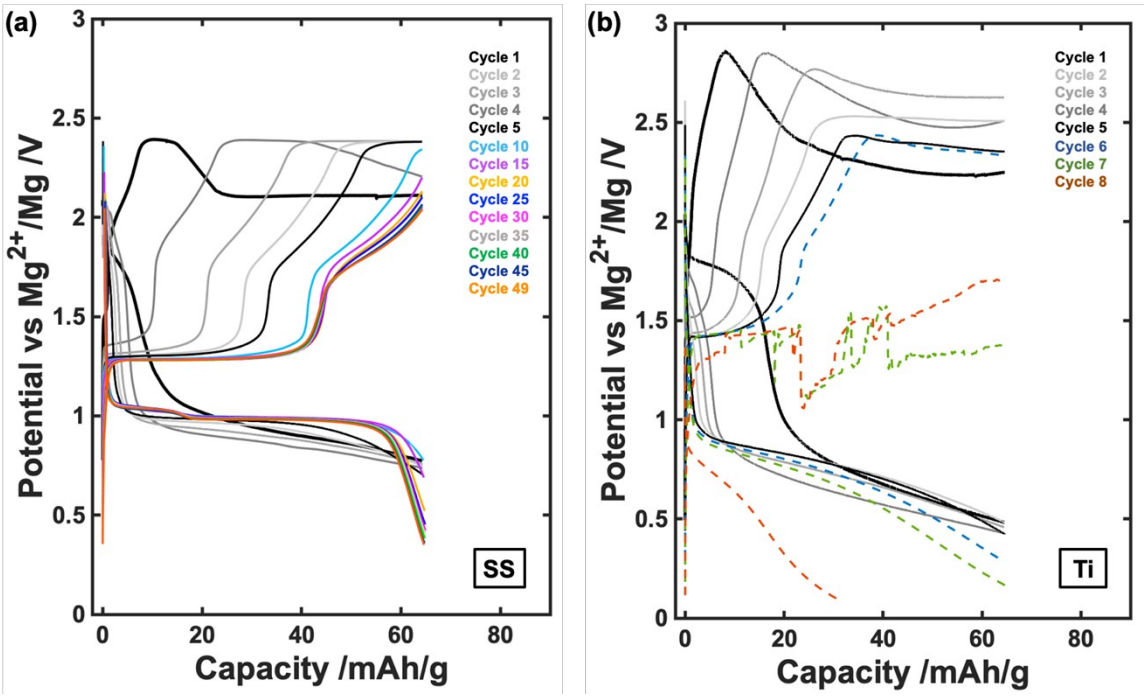

Figure S7: GCPL of Chevrel phase cathode casted on SS foil (full cycles of experiment presented in Figure 7b) in (a), and on Ti foil in (b), showing early degradation. Experiments were done at C/10 rate in 2-electrode Swagelok cells *vs.* Mg metal anode, using 0.4 M $Mg(TFSI)_2$ in DME:DG electrolyte with 40 mM of BI_3.

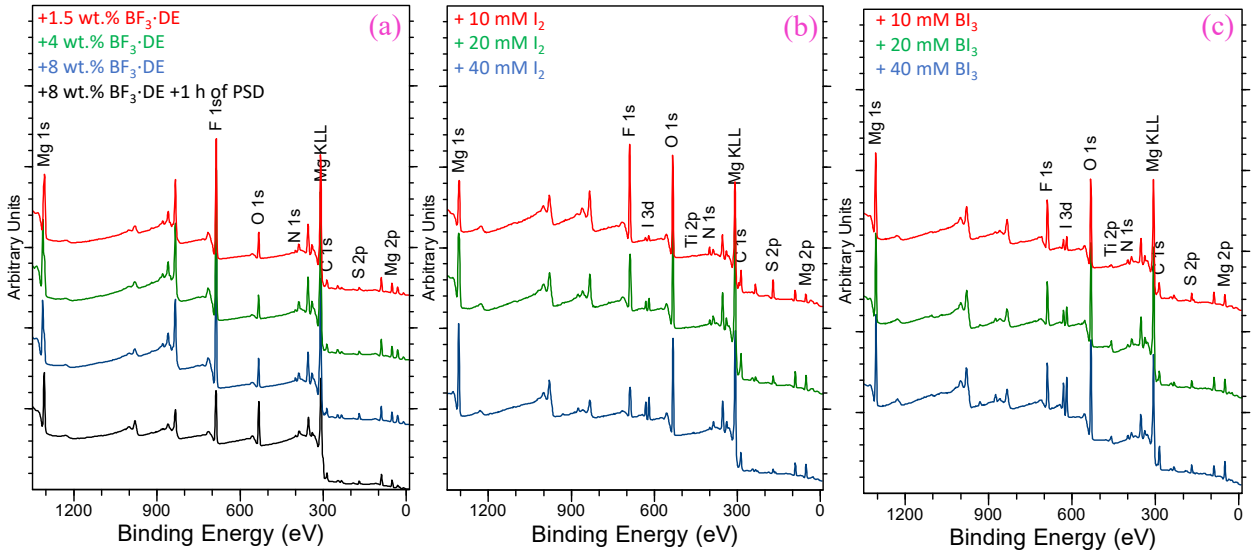

Figure S8: XPS survey spectra of Ti electrodes cycled in the 0.4 M $Mg(TFSI)_2$ in DME:DG electrolyte with adding different amounts of (a) BF_3·DE (b) I_2 (c) BI_3 additives shown in Figures 2, 4 and 6, respectively.

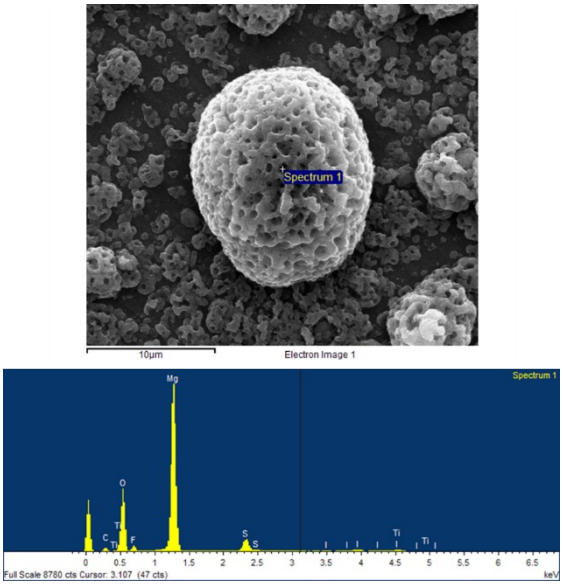

Element	Weight%	Atomic%
C K	9.30	14.52
O K	39.70	46.54
F K	7.78	7.68
Mg K	37.29	28.77
S K	3.33	1.95
Ti K	0.68	0.27
I L	1.91	0.28
Totals	100.00	

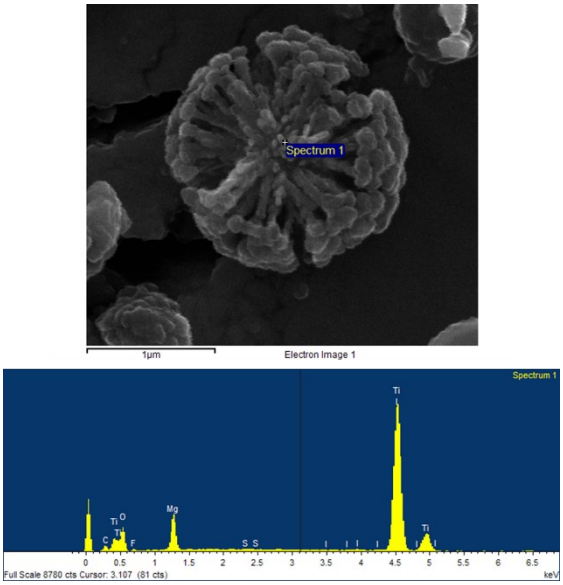

Element	Weight%	Atomic%
C K	4.60	9.45
O K	34.37	53.03
F K	3.45	4.48
Mg K	7.13	7.24
S K	0.14	0.11
Ti K	49.63	25.57
I L	0.69	0.13
Totals	100.00	

Figure S9: Energy Dispersive spectroscopy (EDS) analysis of SEM images of Mg deposits formed on Ti electrodes cycled in 0.4 M $Mg(TFSI)_2$ electrolyte containing 40 mM BI_3 shown in Figure S5.